

Demon driven by geometrical phase

Ryosuke Yoshii*

Center for Liberal Arts and Sciences, Sanyo-Onoda City University, Yamaguchi 756-0884, Japan

Hisao Hayakawa†

Center for Gravitational Physics and Quantum Information,
Yukawa Institute for Theoretical Physics, Kyoto University,
Kitashirakawa-oiwake cho, Sakyo-ku, Kyoto 606-8502, Japan

(Dated: July 12, 2022)

We theoretically study the entropy production and work extracted from a system connected to two reservoirs by periodic modulations of their electrochemical potentials of the reservoirs and one parameter in the system Hamiltonian under isothermal conditions. We find that the modulation of parameters can drive a geometrical state, which is away from a nonequilibrium steady state. With the aid of this property, we construct a demon in which the relative entropy increases with time such that we can extract the work if we begin with the nonequilibrium steady state without parameter modulations. We employ the Anderson model to demonstrate that the relative entropy can increase with time.

Introduction.- The second law of thermodynamics is one of the most fundamental laws in physics, which provides the upper bound of the available work that can be extracted from reservoirs. Maxwell proposed an idealistic setup to violate the second law, in which a demon quickly opens and closes the gate to allow only fast-moving molecules to pass through in one direction [1]. This leads to a decrease in entropy without applying any work, and thus violates the second law of thermodynamics. Because Maxwell's original idea relies on the measurement of molecules, it is natural to combine the physical law and information science with information thermodynamics to realize Maxwell's demon [2–7].

Nevertheless, the cost of implementation of informational Maxwell's demon is expensive, although the theoretical formulation ignores this cost. Instead, we propose a geometrical demon with the aid of Berry's phase [8] in a geometrical engine as an extension of the Thouless pumping [9–11]. We consider a small system sandwiched between two thermal reservoirs. If two parameters in the reservoirs and one parameter in the system Hamiltonian are controlled by an external agent, we can extract the work from the system. This is a natural application of the Thouless pumping [9–25] and geometrical thermodynamics [26–33]. It is known that the Kullback-Leibler (KL) divergence is positive semidefinite, where its zero is only achieved if the system is in a nonequilibrium steady state (NESS) [31, 32, 34–39]. We note that the relative entropy can differ from the KL divergence. Indeed, the KL divergence is always zero for a completely periodic modulation if we start from the NESS at which the KL divergence is zero, because the KL divergence cannot increase for any completely positive and trace-preserving (CPTP) processes [34–39]. However, the relative entropy of a system during a cyclic modulation can be positive

and increase because of the existence of the geometrical phase. Thus, we can extract the work through this geometrical engine with the aid of an increment in the relative entropy.

Geometrical phase and entropy production.- In the present study, we focus on a system connected to two reservoirs. The left and right reservoirs are characterized by electrochemical potentials (μ_L and μ_R) and temperature T , respectively. We choose the control parameters to be the electrochemical potentials in the reservoirs and the confining potential of the system under isothermal conditions.

We modulate the electrochemical potentials through

$$\mu_L = \bar{\mu}(1 + r_L \sin \theta), \quad \mu_R = \bar{\mu}[1 + r_R \sin(\theta + \delta)], \quad (1)$$

where $\bar{\mu} := \frac{1}{2\pi} \int_0^{2\pi} d\theta \mu_\alpha(\theta)$ is the one-cycle average of the electrochemical potential μ_α in a reservoir α ($=L$ or R). We assume that μ_α depends only on the modulation phase θ . We also assume that the system Hamiltonian $\hat{H}(\lambda(\theta))$ is perfectly periodic, i.e., $\hat{H}(\lambda(\theta)) = \hat{H}(\lambda(\theta + 2\pi))$ through a parameter $\lambda(\theta)$, where $\lambda(\theta) := 1 + r_H \cos \theta$. To reduce the number of parameters, we consider only the case when $r := r_L = r_R = r_H$. To maintain the positivity of the parameters, we assume $|r| < 1$. Thus, our system is characterized by a set of fixed parameters such as T and $\bar{\mu}$, and two control parameters, r and δ . To express the control parameters, we introduce $\Lambda(\theta, \delta) := (\lambda(\theta), \mu_L(\theta)/\bar{\mu}, \mu_R(\theta, \delta)/\bar{\mu})$ using Λ_μ as one of its components.

We consider the master equation for the density matrix $\hat{\rho}(\theta, \delta)$:

$$\frac{d}{d\theta} |\hat{\rho}(\theta, \delta)\rangle = \epsilon^{-1} \hat{K} |\hat{\rho}(\theta, \delta)\rangle, \quad (2)$$

where \hat{K} is the evolution operator. We use the vector notation $|\hat{\rho}(\theta, \delta)\rangle$ in Eq. (2), in which the components of the density matrix $\hat{\rho}(\theta, \delta)$ align. Here, we use the scaled time $\theta := \omega t$, where ω is the modulation angular frequency. We also introduce the dimensionless parameter

* e-mail address: ryosuke.yoshii@rs.soc.u.ac.jp

† hisao@yukawa.kyoto-u.ac.jp

ϵ in Eq. (2) as $\epsilon := 2\pi\omega/\Gamma$ where Γ is the bandwidth used to characterize the hopping rate of the electrons from the reservoirs to the system. Introducing the eigenvalue ϵ_i with subscript i for \hat{K} , the corresponding left and right eigenstates $\langle \ell_i |$ and $| r_i \rangle$ satisfy the orthonormal relation $\langle \ell_i | r_j \rangle = \delta_{ij}$, if the eigenvalues are non-degenerate. We assume that there exists a non-degenerate largest eigenvalue $\epsilon_0 := 0$ corresponding to a steady-state. Probability conservation leads to the left-zero eigenvector $\langle \ell_0 |$ defined as $\langle \ell_0 | \hat{K} = 0$ whose diagonal components in the matrix form are 1 and 0 otherwise. The right zero eigenstate $| r_0 \rangle$ satisfying $\hat{K} | r_0 \rangle = 0$ is also expressed as $|\hat{\rho}^{\text{SS}}\rangle$ to specify the NESS.

Because all eigenvalues except $\epsilon_0 = 0$ are negative, the physical state is relaxed to $|\hat{\rho}^{\text{SS}}\rangle$ in the absence of the modulations. This suggests that the natural choice for the initial state would be $|\hat{\rho}^{\text{SS}}\rangle$. The stability of the steady-state has been discussed in Ref. [32].

The entropy production during one-cycle modulation starting from θ is given by

$$\Delta S(\theta, \delta) := S^{\text{HS}}(\hat{\rho}(\theta, \delta) || \hat{\rho}^{\text{SS}}(\theta, \delta)) - S^{\text{HS}}(\hat{\rho}(2\pi + \theta, \delta) || \hat{\rho}^{\text{SS}}(2\pi + \theta, \delta)), \quad (3)$$

where we have introduced the Hatano-Sasa type relative entropy [40]:

$$S^{\text{HS}}(\hat{\rho} || \hat{\sigma}) := \text{Tr} [\hat{\rho} (\ln \hat{\rho} - \ln \hat{\sigma})]. \quad (4)$$

$\Delta S(\theta, \delta)$ in Eq. (3) is expected to be $\Delta S(\theta, \delta) \geq 0$ because the entropy increases with time as $-\dot{S}^{\text{HS}}(\theta, \delta) \geq 0$, where $\dot{S}^{\text{HS}}(\theta, \delta) := (\partial/\partial\theta)S^{\text{HS}}(\theta, \delta)$. Nevertheless, if we begin with the initial condition $\hat{\rho}(0, \delta) = \hat{\rho}^{\text{SS}}(0, \delta)$, Eq. (3) leads to

$$\Delta S(\delta) = -S^{\text{HS}}(\hat{\rho}(2\pi, \delta) || \hat{\rho}^{\text{SS}}(2\pi, \delta)) \leq 0, \quad (5)$$

where hereafter we use $\Delta S(\delta) := \Delta S(\theta = 0, \delta)$, because S^{HS} is positive semidefinite. Note that $S^{\text{HS}}(\theta, \delta)$ decreases towards zero in the absence of the modulation [34–39]. The condition $\Delta S(\delta) \geq 0$ is compatible with Eq. (5) only if $\hat{\rho}(\theta, \delta)$ is always equal to $\hat{\rho}^{\text{SS}}(\theta, \delta)$ for an arbitrary θ . In other words, if the density matrix can differ from $\hat{\rho}^{\text{SS}}(\theta, \delta)$ at some θ , then $\Delta S(\delta)$ is negative. Note that the decrease in entropy can be easily observed in physical situations if we begin with the equilibrium (maximum entropy) state [41].

Assume that the initial state is the steady state $|\hat{\rho}(0, \delta)\rangle = |r_0\rangle = |\hat{\rho}^{\text{SS}}\rangle$. As shown in Refs. [25, 42], we obtain:

$$|\hat{\rho}(\theta, \delta)\rangle \simeq |\hat{\rho}^{\text{SS}}(\theta, \delta)\rangle + \sum_{i \neq 0}^n C_i(\theta, \delta) |r_i(\theta, \delta)\rangle, \quad (6)$$

where

$$C_i(\theta, \delta) = - \int_0^\theta d\phi e^{\epsilon^{-1} \int_\phi^\theta dz \epsilon_i(z, \delta)} \langle \ell_i(\phi, \delta) | \frac{d}{d\phi} |r_0(\phi, \delta)\rangle. \quad (7)$$

Note that the trace preserving is always satisfied for an arbitrary θ from $\langle \ell_0 | r_i \rangle = \delta_{0i}$.

The expressions in Eqs. (6) and (7) are compatible with the slow-modulation approximation employed in Ref. [32]. The leading contribution of the modulation to the entropy production is indicated by the second term on the right-hand side (RHS) of Eq. (6).

Equation (6) is an important relation, because $\hat{\rho}(\theta, \delta)$ deviates from $\hat{\rho}^{\text{SS}}(\theta, \delta)$ if $C_i \neq 0$. Therefore, if C_i for some i is non-zero, the relative entropy S^{HS} is positive. Namely, S^{HS} can increase if the geometrical phase exists. Thus, our system can automatically extract work from the reservoirs. This is the essence of the geometrical demon. Note that the density matrix is reduced to Eqs. (6) and (7) for $\theta \gg 1$, regardless of the initial condition, as shown in Ref. [42], although the geometrical term becomes negligibly small for large θ .

The second term on the RHS of Eq. (6) is the Berry-Sinityn-Nemenman (BSN) connection. For a cyclic modulation satisfying $|r_i(2\pi, \delta)\rangle = |r_i(0, \delta)\rangle$, the deviation from the initial state after one modulation cycle becomes

$$\Delta |\hat{\rho}\rangle := |\hat{\rho}(2\pi, \delta)\rangle - |\hat{\rho}(0, \delta)\rangle = \sum_{i \neq 0} C_i(\delta) |r_i(0, \delta)\rangle, \quad (8)$$

where

$$C_i(\delta) := \int_0^{2\pi} d\phi e^{\epsilon^{-1} \int_\phi^{2\pi} dz \epsilon_i(z, \delta)} \mathcal{A}_i^\mu \frac{\partial \Lambda_\mu}{\partial \phi}. \quad (9)$$

Here, the BSN connection \mathcal{A}_i^μ is defined as

$$\mathcal{A}_i^\mu(\phi, \delta) := -\langle \ell_i(\Lambda(\phi, \delta)) | \frac{\partial}{\partial \Lambda_\mu} |r_0(\Lambda(\phi, \delta))\rangle. \quad (10)$$

According to \mathcal{A}_i^μ , we define the BSN curvature as

$$F_i^{\mu\nu}(\theta, \delta) := \left(\frac{\partial \mathcal{A}_i^\nu}{\partial \Lambda_\mu} \right)_\theta - \left(\frac{\partial \mathcal{A}_i^\mu}{\partial \Lambda_\nu} \right)_\theta. \quad (11)$$

Because of the damping factor in Eq. (9), the contribution of the BSN curvature is localized in time. If the BSN curvature is zero inside the trajectory, we find that $\Delta S(\delta) = 0$, whereas it can be nonzero if any BSN curvature exists. These results can be used if we begin with the general initial condition given in Ref. [42].

Now, we discuss the thermodynamic relations used to construct the geometrical demon. Let us introduce the work $W(\delta)$ as [43, 44]

$$W(\delta) := \int_0^{2\pi} d\theta \mathcal{P}(\theta, \delta), \quad (12)$$

where

$$\mathcal{P}(\theta, \delta) := \text{Tr} \left[\hat{\rho}(\theta, \delta) \frac{\partial \hat{H}(\lambda(\theta))}{\partial \lambda(\theta)} \right] \dot{\lambda}(\theta). \quad (13)$$

The work $W(\delta)$ and power $\mathcal{P}(\theta, \delta)$ can be positive or negative depending on the situation. A positive $\mathcal{P}(\theta, \delta)$

is interpreted as the power supply by the external agent, whereas a negative $\mathcal{P}(\theta, \delta)$ can be regarded as the power loss. One can introduce

$$\mathcal{P}_{A/R}(\theta, \delta) := \frac{\mathcal{P}(\theta, \delta) \pm |\mathcal{P}(\theta, \delta)|}{2}, \quad (14)$$

which satisfies $\mathcal{P}_A(\theta, \delta) = \mathcal{P}(\theta, \delta)$ ($\mathcal{P}_R(\theta, \delta) = -\mathcal{P}(\theta, \delta)$) if $\mathcal{P}(\theta, \delta) > 0$ ($\mathcal{P}(\theta, \delta) < 0$), whereas $\mathcal{P}_A(\theta, \delta) = 0$ ($\mathcal{P}_R(\theta, \delta) = 0$) otherwise. We also introduce $Q_{A/R}$

$$Q_{A/R}(\delta) := \int_0^{2\pi} d\theta \mathcal{P}_{A/R}(\theta, \delta). \quad (15)$$

$Q_A(\delta)$ is interpreted as the absorbing heat of the system, whereas $Q_R(\delta)$ represents the heat released by the system. By definition, there exists a trivial relation $Q_A(\delta) \geq |W(\delta)| \geq W(\delta)$. If the work $W(\delta)$ is negative, the system can be regarded as an engine in which the work done by the system is greater than the work done by the reservoirs. In this situation ($W(\delta) < 0$), we can define the efficiency $\eta(\delta)$ as

$$\eta(\delta) := \frac{|W(\delta)|}{Q_A(\delta)}. \quad (16)$$

Thus, to construct a geometrical demon, we require that $W(\delta) < 0$ to utilize the negative entropy production $\Delta S(\delta) < 0$. To the best of our knowledge, we cannot determine the sign of $W(\delta)$ in general. Therefore, we demonstrate that $W(\delta)$ can be negative using the Anderson model.

Application to the Anderson model.- Let us apply the general framework to the Anderson model for a quantum dot (QD) in which a single dot is coupled to two electron reservoirs [45]. Thus, the total Hamiltonian \hat{H}^{tot} can be written as

$$\hat{H}^{\text{tot}} := \hat{H} + \hat{H}^r + \hat{H}^{\text{int}}, \quad (17)$$

where \hat{H} , reservoir Hamiltonian \hat{H}^r and interaction Hamiltonian \hat{H}^{int} are, respectively, given by

$$\hat{H} = \sum_{\sigma} \epsilon_0 \hat{d}_{\sigma}^{\dagger} \hat{d}_{\sigma} + U(\theta) \hat{n}_{\uparrow} \hat{n}_{\downarrow}, \quad (18)$$

$$\hat{H}^r = \sum_{\alpha, k, \sigma} \epsilon_k \hat{a}_{\alpha, k, \sigma}^{\dagger} \hat{a}_{\alpha, k, \sigma}, \quad (19)$$

$$\hat{H}^{\text{int}} = \sum_{\alpha, k, \sigma} V_{\alpha} \hat{d}_{\sigma}^{\dagger} \hat{a}_{\alpha, k, \sigma} + \text{h.c.}, \quad (20)$$

where $\hat{a}_{\alpha, k, \sigma}^{\dagger}$ and $\hat{a}_{\alpha, k, \sigma}$ are, respectively, the creation and annihilation operators for the electrons in the reservoirs α ($=L$ or R) with the wave number k , energy ϵ_k , and spin σ ($=\uparrow$ or \downarrow). Moreover, $\hat{d}_{\sigma}^{\dagger}$ and \hat{d}_{σ} are those in the QD, and $\hat{n}_{\sigma} = \hat{d}_{\sigma}^{\dagger} \hat{d}_{\sigma}$. $U(\theta) := U_0 \lambda(\theta)$ and V_{α} are, respectively, the time-dependent electron-electron interaction in the QD and the transfer energy between the QD and the

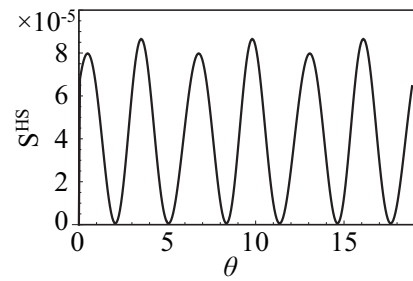


Figure 1. Time evolution of relative entropy $S^{\text{HS}}(\hat{\rho}(\theta, \delta = 0) || \hat{\rho}^{\text{SS}}(\theta, 0))$ for $r = 0.9$ and $\beta U_0 = 0.1$.

reservoir α . We adopt a model in the wide-band limit for the reservoirs. We denote, in this paper, the line width $\Gamma = \pi \varrho (V_L^2 + V_R^2)$, where ϱ is the density of states in the reservoirs.

The Anderson model for the QD has the four states: the double-occupied, singly occupied with an up-spin, singly occupied with a down-spin, and empty. Therefore, the density matrix is expressed as a 4×4 matrix. As shown in Ref. [32], however, $\hat{\rho}(\theta, \delta)$ of the Anderson model under the wideband approximation is reduced to a diagonal matrix, where the diagonal elements correspond to the probability of finding the states in the empty state ρ_e , the down-spin state ρ_{\downarrow} , the up-spin ρ_{\uparrow} , and the double occupied state ρ_d , respectively. The trace-preserving condition $\text{Tr} \hat{\rho} = \rho_e + \rho_{\uparrow} + \rho_{\downarrow} + \rho_d = 1$ reduces to the conservation of probability condition. This implies that the model is a quasi-classical model. The explicit forms of the evolution matrix \hat{K} and the corresponding eigenstates $|\ell_i\rangle$ and $|r_i\rangle$ are summarized in Ref. [42].

For explicit calculation, we use Eqs. (6) and (7), with $\theta = 2\pi$. Integrating by parts, one can show that $C_2(\theta, \delta) = 0$ because $\langle \ell_2 |$ is independent of θ .

One can verify that $\Delta S(\delta) = 0$ for $\beta \epsilon_0 \rightarrow \infty$ [42]. This implies that $\hat{\rho}(\theta, \delta)$ has only a nonzero component ρ_e throughout the process. As a result, the entropy production by the geometrical phase is absent in this limit.

Hereafter, we set $\epsilon = 0.1$ to obtain some explicit results for the Anderson model. Recasting $|\hat{\rho}(\theta)\rangle$ in matrix form $\hat{\rho}(\theta, \delta)$ and plugging it into Eq. (3), we obtain $S^{\text{HS}}(\hat{\rho}(\theta, \delta) || \hat{\rho}^{\text{SS}}(\theta, \delta))$ and ΔS . The time evolution of $S^{\text{HS}}(\hat{\rho}(\theta, \delta) || \hat{\rho}^{\text{SS}}(\theta, \delta))$ is shown in Fig. 1 for $\delta = 0$, $r = 0.9$, and $\beta U_0 = 0.1$. This figure clearly indicates the oscillation of $S^{\text{HS}}(\hat{\rho}(\theta, \delta) || \hat{\rho}^{\text{SS}}(\theta, \delta))$, which increases in some instances. It is easy to verify that all components of $\hat{\rho}(\theta)$ maintain positivity during the dynamics [42], and thus, the dynamics preserve the CPTP. Thus, $S^{\text{HS}}(\hat{\rho}(\theta, \delta) || \hat{\rho}^{\text{SS}}(\theta, \delta))$ cannot be regarded as the KL-divergence. These results are obtained by the BSN connection $C_i(\theta, \delta)$ in Eqs. (6) and (7), all of which are negative definite, as shown in Ref. [42]. We also note that the behavior of $S^{\text{HS}}(\theta, \delta)$ is almost periodic except for the quick relaxation process from the initial condition (see Fig. 1). This indicates that the dynamics are quickly reduced to the quasi-periodic state regardless of the ini-

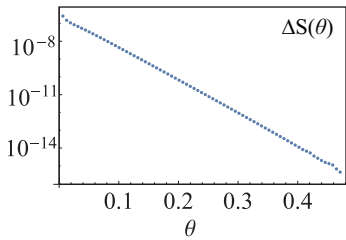


Figure 2. Plots of $\Delta S(\theta, \delta = 0)$ against θ for $\beta U_0 = 0.3$ and $r = 0.9$.

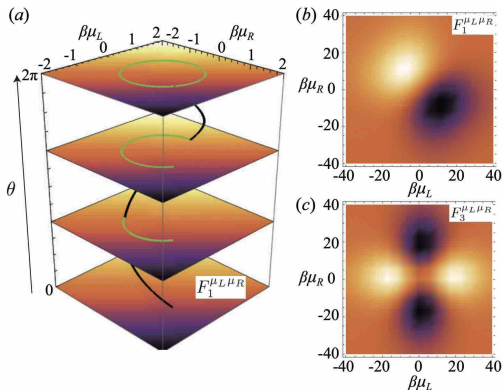


Figure 3. (a) Schematics of a contour of the integral of \mathcal{C}_1 , where the black solid line is the trajectory of the parameters. The color scale at a value of θ expresses $F_1^{\mu_L \mu_R}$. (b) and (c) The BSN curvatures $F_1^{\mu_L \mu_R}$ and $F_3^{\mu_L \mu_R}$ at $\theta = 0$ are plotted. The parameters are set to be $\beta \bar{\mu} = 0.1$, $\beta U_0 = 0.1$ and $\beta \epsilon_0 = 0.1$ for all figures.

tial condition, and thus, $\Delta S(\theta, \delta)$ approaches zero, such that the decay of $\Delta S(\theta, \delta)$ can be approximated by an exponential function of θ , as shown in Fig. 2 [46]. This means that the geometrical term in Eqs. (6) and (7) does not play any role if we start from a quasi-periodic state as in Refs. [32, 42].

Figure 3(a) illustrates the contour of the integral given in Eq. (9) in the parameter space $(\mu_L(\theta), \mu_R(\theta, \delta), \theta)$. As can be seen, the BSN curvature always exists, although its magnitude decreases with θ . The BSN curvatures at specific θ s are plotted in Figs. 3(b) and (c), where the peak (the dip) of $F_1^{\mu_L \mu_R}$ is approximately located at $\beta \mu_R = -\beta \mu_L \approx 10$ ($\beta \mu_R = -\beta \mu_L \approx -10$), whereas the peak (the dip) of $F_3^{\mu_L \mu_R}$ is approximately located at $\beta \mu_L \approx \pm 10, \beta \mu_R = 0$ ($\beta \mu_R \approx \pm 10, \beta \mu_L = 0$).

Figure 4 shows plots of $\Delta S(\delta)$ versus δ for various βU_0 for $r = 0.9$. In this range, the decrement $\Delta S(\delta)$ increases as βU_0 increases.

The work $W(\delta)$ defined in Eq. (12) also becomes negative, as shown in Fig. 5(a). This indicates that we can extract the work by cyclic modulations of the parameters in the Anderson model without fine-tuning. Fig. 5(b), shows the efficiency $\eta(\delta)$ defined in Eq. (16) for one modulation cycle. These results are obtained from $\Delta S(\delta) < 0$;

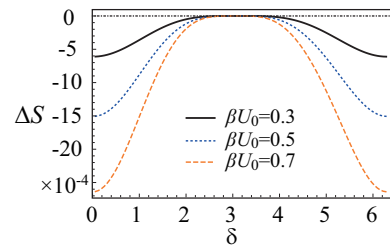


Figure 4. Plots of $\Delta S(\delta)$ versus δ for $\beta U_0 = 0.3$ (solid line), 0.5 (dotted line), 0.7 (dashed line) with fixing $r = 0.9$.

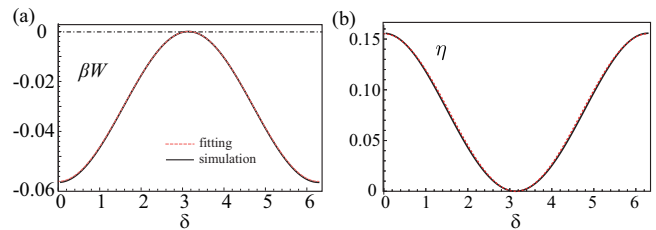


Figure 5. (a) Plots of the work done on the system in one-cycle modulation versus δ with $\beta U_0 = 0.1$ and $r = 0.9$ (solid line) and fitting by the sinusoidal function (dotted line). (b) Plots of the efficiency $\eta(\delta)$ for $\beta U_0 = 0.1$ and $r = 0.9$ (solid line) and fitting by the sinusoidal function (dotted line). The curves for (a) and (b) are fitted by $-0.3(\cos \delta + 1)$ and $0.0766(\cos \delta + 1)$, respectively.

thus, our engine is suitable for calling the geometrical demon.

Concluding Remarks. - We have implemented a geometrical demon through the modulations of the electrochemical potentials in the two reservoirs and the repulsion $U(\theta)$ in the system Hamiltonian under isothermal conditions. We can automatically extract the work from this engine with an increment in relative entropy if we begin with the nonequilibrium steady state. Our geometrical demon does not require any observation of states to decrease the entropy. In this sense, our geometrical demon can be easily implemented in realistic situations; thus, we expect wide applications of this demon, although it does not work after the second cycle. This means that we have to stop the modulation after one cycle, wait until the system reached the NESS again, and then restarted the modulation to extract additional work.

Our future tasks are as follows. (i) Because the present method for the argument is restricted to the case $\epsilon \ll 1$, we will need to extend the analysis to the regime of larger ϵ as done in Ref. [25]. (ii) Although we have analyzed a quantum system, our treatment remains quasi-classical. Thus, we were unable to clarify the role of the quantum coherence [30, 47, 48]. (iii) We ignored the energy cost of controlling $\lambda(\theta)$, $\mu_L(\theta)$, and $\mu_R(\theta, \delta)$; however, it is important to determine this cost when we consider the application of this geometrical demon. The estimation of the cost of controlling parameters is the most important task to be clarified, whereas the contribution of the

housekeeping entropy in our system is positive semidefinite [42].

Acknowledgements.- The authors thank Ville M. M. Paasonen, Kazutaka Takahashi, Kiyoshi Kanazawa, So-

suke Ito, Hikaru Watanabe, and Asahi Yamaguchi for fruitful discussions and useful comments. This study was partially supported by a Grant-in-Aid of MEXT for Scientific Research KAKENHI (Grant Nos. 21H01006, 19K14616 and 20H01838).

-
- [1] J. C. Maxwell, Theory of Heat (Appleton, London, 1871).
- [2] H. Touchette and S. Lloyd, Information-Theoretic Limits of Control. Phys. Rev. Lett. **84**, 1156 (2000).
- [3] T. Sagawa and M. Ueda, Generalized Jarzynski Equality under Nonequilibrium Feedback Control. Phys. Rev. Lett. **104**, 090602 (2010).
- [4] S. Viviana, C.-F. Lee, E. R. Key and D. A. Leigh, A molecular information ratchet, Nature. **445**, 523 (2007).
- [5] S. Toyabe, T. Sagawa, M. Ueda, E. Muneyuki and M. Sano, Experimental demonstration of information-to-energy conversion and validation of the generalized Jarzynski equality, Nature Phys. **6**, 988 (2010).
- [6] J. V. Koski, V. F. Maisi, T. Sagawa, and J. P. Pekola, Experimental Observation of the Role of Mutual Information in the Nonequilibrium Dynamics of a Maxwell Demon, Phys. Rev. Lett. **113**, 030601 (2014).
- [7] J. Parrondo, J. Horowitz and T. Sagawa, Nature Phys. **11**, 131 (2015).
- [8] M. V. Berry, Quantal phase factors accompanying adiabatic changes, Proc. R. Soc. London Ser. A **392**, 45 (1984).
- [9] D. J. Thouless, Quantization of particle transport, Phys. Rev. B **27**, 6083 (1983).
- [10] N. A. Sinitsyn and I. Nemenman, The Berry phase and the pump flux in stochastic chemical kinetics, Europhys. Lett. **77**, 58001 (2007).
- [11] N. A. Sinitsyn and I. Nemenman, Universal Geometric Theory of Mesoscopic Stochastic Pumps and Reversible Ratchets, Phys. Rev. Lett. **99**, 220408 (2007).
- [12] L. P. Kouwenhoven, A. T. Johnson, N. C. van der Vaart, C. J. P. M. Harmans, and C. T. Foxon, Quantized current in a quantum-dot turnstile using oscillating tunnel barriers, Phys. Rev. Lett. **67**, 1626 (1991).
- [13] H. Pothier, P. Lafarge, C. Urbina, D. Esteve, and M. H. Devoret, Single-Electron Pump Based on Charging Effects, Europhys. Lett. **17**, 249 (1992).
- [14] M. Switkes, C. M. Marcus, K. Campman, and A. C. Gossard, An Adiabatic Quantum Electron Pump, Science **283**, 1905 (1999).
- [15] A. Fuhrer, C. Fasth, and L. Samuelson, Single electron pumping in InAs nanowire double quantum dots, Appl. Phys. Lett. **91**, 052109 (2007).
- [16] S. K. Watson, R. M. Potok, C. M. Marcus, and V. Umansky, Experimental Realization of a Quantum Spin Pump, Phys. Rev. Lett. **91**, 258301 (2003).
- [17] P. W. Brouwer, Scattering approach to parametric pumping, Phys. Rev. B **58**, R10135 (1998).
- [18] J. Ren, P. Hänggi, and B. Li, Berry-Phase-Induced Heat Pumping and Its Impact on the Fluctuation Theorem, Phys. Rev. Lett. **104**, 170601 (2010).
- [19] T. Sagawa and H. Hayakawa, Geometrical expression of excess entropy production, Phys. Rev. E **84**, 051110 (2011).
- [20] T. Yuge, T. Sagawa, A. Sugita, and H. Hayakawa, Geometrical pumping in quantum transport: Quantum master equation approach, Phys. Rev. B **86**, 235308 (2012).
- [21] T. Yuge, T. Sagawa, A. Sugiura, and H. Hayakawa, Geometrical Excess Entropy Production in Nonequilibrium Quantum Systems, J. Stat. Phys. **153**, 412 (2013).
- [22] K. L. Watanabe and H. Hayakawa, Geometric fluctuation theorem for a spin-boson system, Phys. Rev. E **96**, 022118 (2017).
- [23] Y. Hino and H. Hayakawa, Fluctuation relations for adiabatic pumping, Phys. Rev. E **102**, 012115 (2020).
- [24] K. Takahashi, Y. Hino, K. Fujii and H. Hayakawa, Full Counting Statistics and Fluctuation?Dissipation Relation for Periodically Driven Two-State Systems, J. Stat. Phys. **181**, 2206 (2020).
- [25] K Takahashi, K Fujii, Y Hino, and H Hayakawa, Nonadiabatic Control of Geometric Pumping, Phys. Rev. Lett. **124**, 150602 (2020).
- [26] Z. Wang, L. Wang, J. Chen, C. Wang and J. Rie, Geometric heat pump: Controlling thermal transport with time-dependent modulations Frontier, Phys. **17**, 13201 (2022).
- [27] G. E. Crooks, Measuring Thermodynamic Length, Phys. Rev. Lett. **99**, 100602 (2007).
- [28] B. Bhandari, P. T. Alonso, F. Taddei, F. von Oppen, R. Fazio and L. Arrachea, Geometric properties of adiabatic quantum thermal machines, Phys. Rev. B **102**, 155407 (2020),
- [29] P Abiuso, H. J. D. Miller, M. Perarnau-Llobet, and M Scandi, Geometric optimisation of quantum thermodynamic processes, Entropy **22**, 1076 (2020).
- [30] K. Brandner and K. Saito, Thermodynamic Geometry of Microscopic Heat Engines, Phys. Rev. Lett. **124**, 040602 (2020).
- [31] Y. Hino and H. Hayakawa, Geometrical formulation of adiabatic pumping as a heat engine, Phys. Rev. Research **3**, 013187 (2021).
- [32] H. Hayakawa, V. M. M. Paasonen, and R. Yoshii, “Geometrical Quantum Chemical Engine”, arXiv:2112.12370 (2021).
- [33] J. Lu, Z. Wang, J. Peng, C. Wang, J.-H. Jiang and J. Ren, Geometric thermodynamic uncertainty relation in a periodically driven thermoelectric heat engine Phys, Rev. B. **105**, 115428 (2022).
- [34] S. Kullback, and R. A. Leibler, On information and sufficiency, Annal. Math. Stat., **22**, 79 (1951).
- [35] T. Sagawa, Entropy, Divergence, and Majorization in Classical and Quantum Thermodynamics, to be published in Springer-Brief in Mathematical Physics arXiv:2007.09974.
- [36] D. Petz, Quasi-entropies for finite quantum systems, Rep. Math. Phys. **23**, 57 (1986).
- [37] D. Petz, Monotonicity of quantum relative entropy revisited, Rev. Math. Phys. **15**, 79 (2003)
- [38] M. B. Ruskai, Inequalities for quantum entropy: A review with conditions for equality, J. Math. Phys. **43**, 4358 (2002).

- [39] F. Hiai, M. Mosonyi, D. Petz, and C. Bény, Quantum f-divergences and error correction, *Rev. Math. Phys.* **23**, 691 (2011).
- [40] T. Hatano and S.-i. Sasa, Steady-State Thermodynamics of Langevin Systems, *Phys. Rev. Lett.* **86**, 3463 (2001).
- [41] As can be seen in the relation $S^{\text{HS}}(\hat{\rho}^{\text{SS}}(\theta)||\hat{\rho}^{\text{SS}}(\theta)) = 0$, our formulation has already eliminated the energy supply (from the connection with higher electrochemical potential) and dissipation (from the connection with the lower electrochemical potential) terms, which are perfectly balanced with each other in the nonequilibrium steady state. Thus, the Joule heat term does not appear explicitly in our formulation. See Ref. [42] for the role of the housekeeping entropy.
- [42] See Supplemental Material.
- [43] G. Benenti, G. Casati, K. Saito, and R. S. Whitney, *Phys. Rep.* **694**, 1 (2017).
- [44] G. Kurizki and A. G. Kofman, *Thermodynamics and Control of Open Quantum Systems* (Cambridge Univ. Press, Cambridge, 2022).
- [45] Though there exist higher energy levels in realistic quantum dot systems, here we only consider the single energy level for simplicity.
- [46] Needless to say, the system with $\Delta S < 0$ is not perfectly periodic even if $\hat{H}(\lambda(\theta))$ and the control parameters are periodic. Since there exists a damping factor in the geometrical contribution, $|\Delta S|$ in the second cycle is much smaller than that in the first cycle as explained in the main text. In the long time limit, the system asymptotically reaches the NESS in which the geometrical contribution asymptotically is negligible.
- [47] A. A. Svidzinsky, K. E. Dorfman, M. O. Scully, Enhancing photocell power by noise-induced coherence, *Coherent Opt. Phenomena*, **1**, 7 (2012).
- [48] J. Um, K. E. Dorfman and H. Park, Coherence enhanced quantum-dot heat engine, arXiv:2111.09582.

This Supplemental Material explains the details of calculations that are not included in the main text. In Sec. I we derive a general expression for the time evolution of the density matrix $\hat{\rho}(\theta, \delta)$ without a specific choice of model and initial condition. In Sec. II we explain the contribution of the housekeeping entropy, which has been ignored in the main text. In Sec. III we present the detailed properties of the Anderson model. In Sec. IV we briefly summarize the differences between our analysis and the analysis in Ref. [S1].

I. TIME EVOLUTION OF THE DENSITY MATRIX

This section consists of two subsections. In the first part, IA, we derive the time evolution of $\hat{\rho}(\theta, \delta)$ from the general initial condition to demonstrate the universality of Eqs. (6) and (7) for $\theta \gg 1$. In the second part, IB, we present the detailed derivations of the BSN connection and BSN curvature.

A. Derivation of the time-dependent expression of the density matrix starting from the general initial condition

The purpose of this section is to derive Eqs. (6) and (7). Although we assumed that the initial state is given by $\hat{\rho}^{\text{SS}}(\theta = 0, \delta)$ in the main text, we can derive these equations even when we begin with the generalized initial condition

$$|\hat{\rho}_{\text{ini}}\rangle = \sum_i a_i |r_i(0, \delta)\rangle, \quad (\text{S1})$$

where a_i is given by

$$a_i := \langle \ell_i(0, \delta) | \hat{\rho}_{\text{ini}} \rangle. \quad (\text{S2})$$

We note that the normalization of the density matrix fixes the coefficient a_0 to 1, because

$$\text{Tr} \hat{\rho}_{\text{ini}} = \langle \ell_0 | \hat{\rho}_{\text{ini}} \rangle = \sum_i a_i \langle \ell_0 | r_i(0, \delta) \rangle = a_0 = 1. \quad (\text{S3})$$

One can derive $|\hat{\rho}(\theta, \delta)\rangle$ for $|\hat{\rho}(0, \delta)\rangle = |\hat{\rho}_{\text{ini}}\rangle$ as

$$\begin{aligned} & |\hat{\rho}(\theta + \Delta\theta, \delta)\rangle \\ & \simeq \sum_{i,j,k,\dots,l,m} a_m |r_i(\theta, \delta)\rangle e^{\varepsilon_i(\theta, \delta) \frac{\Delta\theta}{\varepsilon}} \langle \ell_i(\theta, \delta) | r_j(\theta - \Delta\theta, \delta)\rangle \\ & \quad \times e^{\varepsilon_j(\theta - \Delta\theta, \delta) \frac{\Delta\theta}{\varepsilon}} \langle \ell_j(\theta - \Delta\theta, \delta) | r_k(\theta - 2\Delta\theta, \delta)\rangle \\ & \quad \dots \times e^{\varepsilon_l(\Delta\theta)} \langle \ell_l(0, \delta) | r_m(0, \delta)\rangle \\ & = \sum_m a_m e^{\int_0^\theta \varepsilon_m(\phi, \delta) \frac{d\phi}{\varepsilon}} |r_m(\theta, \delta)\rangle + \sum_{m,n} C_{mn} a_n |r_m(\theta, \delta)\rangle, \end{aligned} \quad (\text{S4})$$

where C_{mn} is given by

$$C_{mn}(\theta, \delta) = - \int_0^\theta d\phi e^{\int_\phi^\theta \varepsilon_m(\xi, \delta) \frac{d\xi}{\epsilon}} e^{\int_0^\phi \varepsilon_n(\zeta, \delta) \frac{d\zeta}{\epsilon}} \times \langle \ell_m(\phi, \delta) | \frac{d}{d\phi} | r_n(\phi, \delta) \rangle. \quad (\text{S5})$$

The phase factor in the first term on the RHS of Eq. (S4) is the dynamical phase, whereas the second term on the RHS is the term generated by the geometrical phase. Substituting $\int_\phi^\theta \varepsilon_m(\xi, \delta) \frac{d\xi}{\epsilon} = \int_0^\theta \varepsilon_m(\xi, \delta) \frac{d\xi}{\epsilon} - \int_0^\phi \varepsilon_m(\xi, \delta) \frac{d\xi}{\epsilon}$ in Eq. (S5) and substituting this result into Eq. (S4), we obtain

$$|\hat{\rho}(\theta, \delta)\rangle \simeq \sum_m a_m |\tilde{r}_m(\theta, \delta)\rangle + \sum_{m,n} \tilde{C}_{mn} a_n |\tilde{r}_m(\theta, \delta)\rangle, \quad (\text{S6})$$

where we have introduced

$$\tilde{C}_{mn}(\theta, \delta) := - \int_0^\theta d\phi \langle \tilde{\ell}_m(\phi, \delta) | \left(\frac{d}{d\phi} - \frac{\varepsilon_n}{\epsilon} \right) |\tilde{r}_n(\phi, \delta)\rangle, \quad (\text{S7})$$

$$|\tilde{r}_m(\theta, \delta)\rangle := e^{\int_0^\theta \varepsilon_m(\phi, \delta) \frac{d\phi}{\epsilon}} |r_m(\theta, \delta)\rangle, \quad (\text{S8})$$

and

$$\langle \tilde{\ell}_m(\theta, \delta) | := \langle \ell_m(\theta, \delta) | e^{-\int_0^\theta \varepsilon_m(\phi) \frac{d\phi}{\epsilon}}. \quad (\text{S9})$$

The orthonormal relation $\langle \ell_m | r_n \rangle = \delta_{mn}$ leads to

$$\langle \tilde{\ell}_m(\theta, \delta) | \tilde{r}_n(\theta, \delta) \rangle = e^{-\int_0^\theta \varepsilon_m(\phi, \delta) \frac{d\phi}{\epsilon}} e^{\int_0^\theta \varepsilon_n(\phi, \delta) \frac{d\phi}{\epsilon}} \delta_{mn} = \delta_{mn}. \quad (\text{S10})$$

Substituting this relation into Eq. (S7), we obtain

$$\tilde{C}_{mn}(\theta, \delta) = \frac{\delta_{mn}}{\epsilon} \int_0^\theta d\phi \varepsilon_n(\phi, \delta) - \int_0^\theta d\phi \langle \tilde{\ell}_m(\phi, \delta) | \frac{d}{d\phi} |\tilde{r}_n(\phi, \delta)\rangle. \quad (\text{S11})$$

Equations (S6) and (S11) are expressions of the time evolution starting from the general initial condition in Eq. (S1).

Note that the trace of $\hat{\rho}(\theta, \delta)$ is always equal to unity. This can be proven as follows. The coefficient C_{0j} identically vanishes because

$$\begin{aligned} \langle \tilde{\ell}_0(\phi, \delta) | \frac{\partial}{\partial \Lambda_\mu} |\tilde{r}_j(\phi, \delta)\rangle &= \frac{\partial \langle \tilde{\ell}_0(\phi, \delta) |}{\partial \Lambda_\mu} |\tilde{r}_j(\phi, \delta)\rangle \\ &\quad - \frac{\partial}{\partial \Lambda_\mu} \langle \tilde{\ell}_0(\phi, \delta) | \tilde{r}_j(\phi, \delta) \rangle \\ &= 0. \end{aligned} \quad (\text{S12})$$

Thus, $\text{Tr} \hat{\rho}(\theta, \delta)$ satisfies

$$\text{Tr} \hat{\rho}(\theta, \delta) = \langle \ell_0 | \hat{\rho}(\theta, \delta) \rangle = a_0 = 1, \quad (\text{S13})$$

where we have used $\varepsilon_0(\phi, \delta) = 0$ and Eq. (S10) to obtain this result.

Now, let us consider the behavior for $\theta/\epsilon \gg 1$. It is evident that the first term on the RHS of Eq. (S6) is reduced to $|\hat{\rho}^{\text{SS}}(\theta)\rangle$ because the exponential damping factor for $m \neq 0$ is negligible. Thus, Eq. (S6) is reduced to

$$|\hat{\rho}(\theta)\rangle \simeq |\hat{\rho}^{\text{SS}}(\theta, \delta)\rangle + \sum_{m,n} C_{mn}(\theta, \delta) a_n |r_m(\theta, \delta)\rangle \quad (\text{S14})$$

for $\theta/\epsilon \gg 1$. It is straightforward to evaluate $C_{mn}(\theta, \delta)$ for $n \neq 0$ as

$$\begin{aligned} |C_{mn}(\theta)| &= \left| \int_0^\theta d\phi e^{\int_\phi^\theta \varepsilon_m(\xi) \frac{d\xi}{\epsilon}} e^{\int_0^\phi \varepsilon_n(\zeta) \frac{d\zeta}{\epsilon}} \langle \ell_m(\phi) | \frac{d}{d\phi} | r_n(\phi) \rangle \right| \\ &\leq \int_0^\theta d\phi e^{\int_\phi^\theta \varepsilon_m(\xi) \frac{d\xi}{\epsilon}} e^{\int_0^\phi \varepsilon_n(\zeta) \frac{d\zeta}{\epsilon}} \left| \langle \ell_m(\phi) | \frac{d}{d\phi} | r_n(\phi) \rangle \right| \\ &\leq \int_0^\theta d\phi e^{\int_0^\theta \max(\varepsilon_m, \varepsilon_n)(\xi) \frac{d\xi}{\epsilon}} \left| \langle \ell_m(\phi) | \frac{d}{d\phi} | r_n(\phi) \rangle \right|, \end{aligned} \quad (\text{S15})$$

where we have omitted δ dependence in the expressions in Eq. (S15). Thus, C_{mn} with $n \neq 0$ is much smaller than C_{m0} because of the existence of the exponential factor in Eq. (S15).

Equation (S14) implies that the relative entropy $\Delta S(\theta, \delta)$ approaches 0 in the absence of the geometrical phase, but not in the presence of the geometrical phase. Moreover, the relative entropy becomes non-zero, as indicated by the results in the main text. Thus, the geometrical phase prevents the system from the relaxation towards the NESS (at which the relative entropy S^{HS} is zero). Once we start to modulate the parameters, the system is driven from the NESS state. However, because of the exponential factor in Eq. (S5), which truncates the contribution in the integration except for $\phi \approx \theta$, the system again exhibits periodic behavior in θ after the characteristic time given by the eigenvalues of \hat{K} . As a result, the relative entropy S^{HS} also becomes periodic in θ after some characteristic time θ_c . Thus the relative entropy $\Delta S(\theta, \delta)$ is expected to be zero for $\theta > \theta_c$. In Fig. 2, we plot the θ dependence of $\Delta S(\theta, \delta)$, which clearly shows that $\Delta S(\theta, \delta)$ exponentially approaches zero.

B. Derivation of BSN connection and BSN curvature

For the cyclic modulation $|r_i(2\pi, \delta)\rangle = |r_i(0, \delta)\rangle$, the time evolution from the general initial state becomes

$$\begin{aligned} \Delta |\hat{\rho}\rangle &= \sum_{i \neq 0} a_i \left(e^{\int_0^{2\pi} \varepsilon_i(\phi, \delta) \frac{d\phi}{\epsilon}} - 1 \right) |r_i(0, \delta)\rangle \\ &\quad + \sum_{i,j} C_{ij} a_j e^{\int_0^{2\pi} \varepsilon_i(\phi, \delta) \frac{d\phi}{\epsilon}} |r_i(0, \delta)\rangle, \end{aligned} \quad (\text{S16})$$

where

$$\mathcal{C}_{ij} := \delta_{ij} \oint_{\partial\Omega} d\phi \frac{\varepsilon_i(\phi, \delta)}{\epsilon} - \int_{\partial\Omega} d\Lambda_\mu \mathcal{A}_{ij}^\mu \quad (\text{S17})$$

with the introduction of the BSN connection \mathcal{A}_{ij}^μ :

$$\mathcal{A}_{ij}^\mu := \langle \tilde{\ell}_i(\phi, \delta) | \frac{\partial}{\partial \Lambda_\mu} | \tilde{r}_j(\phi, \delta) \rangle. \quad (\text{S18})$$

Here, the summation of the first term on the RHS of Eq. (S16) is considered except for $i = 0$ because $\varepsilon_0(\phi, \delta) = 0$ always yields $e^{\int_0^\theta \varepsilon_0(\phi, \delta) \frac{d\phi}{\epsilon}} = 1$. Using the Stokes theorem, we can rewrite Eq. (S17) as

$$\mathcal{C}_{ij} = \delta_{ij} \oint_{\partial\Omega} d\phi \frac{\varepsilon_i(\phi, \delta)}{\epsilon} - \int_{\Omega} dS_{\mu\nu} F_{ij}^{\mu\nu}, \quad (\text{S19})$$

where Ω is the area enclosed by the closed trajectory $\partial\Omega$, $S_{\mu\nu} = \frac{1}{2} d\Lambda_\mu \wedge d\Lambda_\nu$, and $F_{ij}^{\mu\nu}$ represents the BSN curvatures defined as

$$F_{ij}^{\mu\nu} := \frac{\partial \langle \tilde{\ell}_i |}{\partial \Lambda_\nu} \frac{\partial | \tilde{r}_j \rangle}{\partial \Lambda_\mu} - \frac{\partial \langle \tilde{\ell}_i |}{\partial \Lambda_\mu} \frac{\partial | \tilde{r}_j \rangle}{\partial \Lambda_\nu}. \quad (\text{S20})$$

It is also possible to rewrite Eq. (S19) as

$$\mathcal{C}_{ij} = \delta_{ij} \oint_{\partial\Omega} d\phi \frac{\varepsilon_i(\phi, \delta)}{\epsilon} + \frac{1}{2} \int_{\Omega} d\langle \tilde{\ell}_i | \wedge d | \tilde{r}_j \rangle. \quad (\text{S21})$$

II. CONTRIBUTION OF THE HOUSEKEEPING ENTROPY

The nonequilibrium system we consider is sustained by an external agent, which requires housekeeping heat as well as excess heat, although the main text only contains the description for the excess heat [S2, S3]. In this section, we evaluate the housekeeping entropy production in our system.

As shown in Refs. [S2, S3], we introduce a set of counting fields χ to calculate physical observables. As a result, Eq. (2) is formally modified as

$$\frac{d}{d\theta} |\hat{\rho}(\theta, \delta, \chi)\rangle = \epsilon^{-1} \hat{K}^\chi |\hat{\rho}(\theta, \delta, \chi)\rangle, \quad (\text{S22})$$

where the set of counting fields contains two components $\chi = (\chi_L, \chi_R)$, which are inserted to monitor the time evolution of the housekeeping entropy production in the left and right lead, respectively, and $|\hat{\rho}(\theta, \delta, \chi)\rangle$ and \hat{K}^χ are the generalized density matrix and the evolution operator, respectively. Since $|\hat{\rho}(\theta, \delta, \chi)\rangle$ behaves as $|\hat{\rho}(\theta, \delta, \chi)\rangle \sim \exp[\lambda_0(\mathbf{\Lambda}, \chi)\theta/\epsilon]$ for large θ/ϵ with the smallest eigenvalue $\lambda_0(\mathbf{\Lambda}, \chi)$ of \hat{K}^χ (which is reduced to zero in the limit $\chi \rightarrow \mathbf{0}$) under a fixed $\mathbf{\Lambda}$, the housekeeping entropy flux [S2, S3] is given by

$$J_{\text{hk}}(\phi, \delta) := \left. \frac{\partial \lambda_0(\mathbf{\Lambda}(\phi, \delta), \chi)}{\partial (i\chi_L)} \right|_{\chi=\mathbf{0}} + \left. \frac{\partial \lambda_0(\mathbf{\Lambda}(\phi, \delta), \chi)}{\partial (i\chi_R)} \right|_{\chi=\mathbf{0}}. \quad (\text{S23})$$

Note that χ_L and χ_R couple to the housekeeping entropy production in the left reservoir ($\hat{\mathcal{S}}_L = \beta(\hat{H}_L - \mu_L)$) and that in the right reservoir ($\hat{\mathcal{S}}_R = \beta(\hat{H}_R - \mu_R)$), respectively, where \hat{H}_α ($\alpha = L, R$) stands for the Hamiltonian of the reservoir α . This housekeeping entropy flux is dominant to maintain the steady-state.

More explicitly, \hat{K}^χ in Eq. (S22) can be written as

$$\hat{K}^\chi = \hat{K} + i \sum_{\alpha=L,R} \chi_\alpha \hat{\mathcal{K}}_\alpha + O(\chi^2). \quad (\text{S24})$$

For the explicit calculation of Eq. (S23), we employ the Anderson model, as in the main text. In the following, we consider the generating function defined by

$$\ln \text{Tr} \rho(\theta, \delta, \chi) = \ln \left\langle e^{i(\chi_L \hat{\mathcal{S}}_L(\theta) + \chi_R \hat{\mathcal{S}}_R(\theta, \delta))} \right\rangle, \quad (\text{S25})$$

where the bracket stands for the thermal and quantum averages. In the present case, only \hat{H}^{int} in the total hamiltonian does not commute with $e^{i(\chi_L \hat{\mathcal{S}}_L + \chi_R \hat{\mathcal{S}}_R)}$. In this case, one can use the technique with that used in Ref. [S4], namely, the counting fields can be absorbed as the phases of the interaction part.

$$e^{-i\frac{\chi}{2} \hat{\mathcal{S}}_\alpha} V_\beta d_\sigma^\dagger a_{\beta,k,\sigma} e^{i\frac{\chi}{2} \hat{\mathcal{S}}_\alpha} = e^{i\frac{\chi}{2} \mathfrak{S}_{\alpha,k} \delta_{\alpha\beta}} V_\beta d_\sigma^\dagger a_{\beta,k,\sigma}, \quad (\text{S26})$$

$$e^{-i\frac{\chi}{2} \hat{\mathcal{S}}_\alpha} V_\beta a_{\beta,k,\sigma}^\dagger d_\sigma e^{i\frac{\chi}{2} \hat{\mathcal{S}}_\alpha} = e^{i\frac{\chi}{2} \mathfrak{S}_{\alpha,k} \delta_{\alpha\beta}} V_\beta a_{\beta,k,\sigma}^\dagger d_\sigma, \quad (\text{S27})$$

where $\mathfrak{S}_{\alpha,k} = \beta(\epsilon_k - \mu_\alpha)$ and $\delta_{\alpha\beta}$ is Kronecker's delta. Then, we just need to proceed the following transposition to calculate the generating function.

$$a_{\alpha,k,\sigma}^\dagger \rightarrow e^{i\frac{\chi_\alpha}{2} \mathfrak{S}_{\alpha,k}} a_{\alpha,k,\sigma}^\dagger, \quad (\text{S28})$$

$$a_{\alpha,k,\sigma} \rightarrow e^{-i\frac{\chi_\alpha}{2} \mathfrak{S}_{\alpha,k}} a_{\alpha,k,\sigma}. \quad (\text{S29})$$

As a consequence, the similar calculation in Ref. [S4] yields \hat{K}^χ as

$$\hat{K}^\chi = \Gamma \begin{pmatrix} -2f_-^{(1)} & f_+^{(1)\chi} & f_+^{(1)\chi} & 0 \\ f_-^{(1)\chi} & -f_+^{(0)} - f_+^{(1)} & 0 & f_+^{(0)\chi} \\ f_-^{(1)\chi} & 0 & -f_+^{(0)} - f_+^{(1)} & f_+^{(0)\chi} \\ 0 & f_-^{(0)\chi} & f_-^{(0)\chi} & -2f_+^{(0)} \end{pmatrix}, \quad (\text{S30})$$

where $f_+^{(j)\chi} = e^{i\chi_L \mathfrak{S}_L^j} f_L^{(j)}(\epsilon_0) + e^{i\chi_R \mathfrak{S}_R^j} f_R^{(j)}(\epsilon_0)$ and $f_-^{(j)\chi} = e^{-i\chi_L \mathfrak{S}_L^j} [1 - f_L^{(j)}(\epsilon_0)] + e^{-i\chi_R \mathfrak{S}_R^j} [1 - f_R^{(j)}(\epsilon_0)]$, $\mathfrak{S}_\alpha^j = \beta(\epsilon_0 + jU - \mu_\alpha)$. Here, $f_\alpha^{(j)}(\epsilon_0) = [1 + e^{\beta(\epsilon_0 + jU - \mu_\alpha)}]^{-1}$ corresponds to the Fermi distribution function. Substituting Eq. (S30) into Eq. (S24), we can write $\hat{\mathcal{K}}_\alpha$ as

$$\hat{\mathcal{K}}_\alpha = \begin{pmatrix} 0 & S_\alpha^1 g_\alpha^1 & S_\alpha^1 g_\alpha^1 & 0 \\ S_\alpha^1 (g_\alpha^1 - 1) & 0 & 0 & S_\alpha^0 g_\alpha^0 \\ S_\alpha^1 (g_\alpha^1 - 1) & 0 & 0 & S_\alpha^0 g_\alpha^0 \\ 0 & S_\alpha^0 (g_\alpha^0 - 1) & S_\alpha^0 (g_\alpha^0 - 1) & 0 \end{pmatrix}, \quad (\text{S31})$$

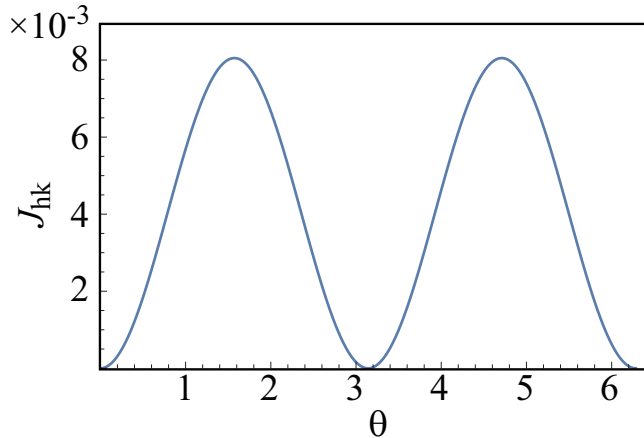


Figure S6. Time dependence of housekeeping entropy production flux J_{hk} . Here we set $r = 0.9$ $\delta = \pi$, and $\beta U_0 = 0.1$.

with $g_\alpha^j := (1 + e^{\beta(\epsilon_0 + jU - \mu_\alpha)})^{-1}$, $S_\alpha^j = \beta(\mu_\alpha - \epsilon_0 - jU)$ ($j = 1, 2$, $\alpha = L, R$). Using the relation

$$\lambda_{0,\alpha}^{(1)}(\mathbf{\Lambda}(\phi, \delta)) = \langle \ell_0 | \hat{\mathcal{K}}_\alpha(\mathbf{\Lambda}(\phi, \delta)) | r_0 \rangle. \quad (\text{S32})$$

and the expansion

$$\lambda_0(\mathbf{\Lambda}(\phi, \delta), \boldsymbol{\chi}) = i \sum_\alpha \chi_\alpha \lambda_{0,\alpha}^{(1)}(\mathbf{\Lambda}(\phi, \delta)) + O(\chi^2), \quad (\text{S33})$$

we obtain $\lambda_0(\mathbf{\Lambda}, \boldsymbol{\chi})$ and J_{hk} .

The housekeeping entropy production during one cycle is given by

$$S_{\text{hk}}(\theta, \delta) := \int_\theta^{\theta+2\pi} d\phi J_{\text{hk}}(\phi, \delta). \quad (\text{S34})$$

Substituting Eqs. (S23), (S32) and (S33) into Eq. (S34), we obtain

$$S_{\text{hk}}(\theta, \delta) = \sum_{\alpha=L,R} \int_\theta^{\theta+2\pi} d\phi \langle \ell_0 | \hat{\mathcal{K}}_\alpha(\mathbf{\Lambda}(\phi, \delta)) | r_0 \rangle. \quad (\text{S35})$$

We note that $S_{\text{hk}}(\theta, \delta)$ is independent of θ , because $\lambda_0(\mathbf{\Lambda}(\phi), \boldsymbol{\chi})$ depends on ϕ only through $\mathbf{\Lambda}(\phi, \delta)$ which is a periodic function of ϕ . In Fig. S6, we plot the time dependence of the housekeeping entropy production given by Eq. (S23) in the case of the Anderson model, where we set $\delta = \pi$. The housekeeping entropy production is always non-negative as it is expected. We also plot the housekeeping entropy production during one cycle as a function of δ in Fig. S7. As shown in Fig. S7, the housekeeping entropy production during one cycle is positive irrespective of δ , except for $\delta = 0$. In the case of $\delta = 0$, the average bias voltage is absent and thus the housekeeping entropy production, which maintain the steady-state, is zero.

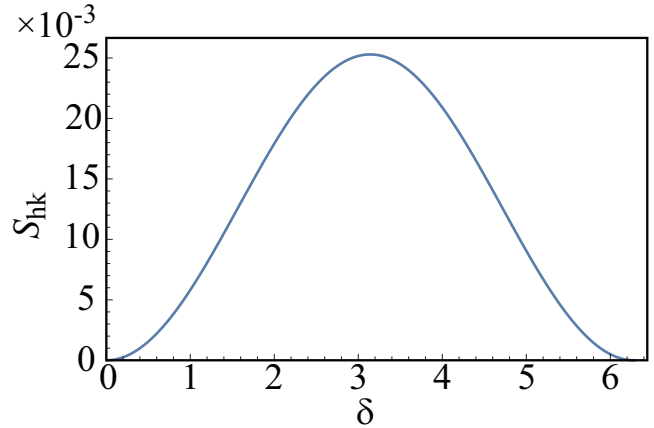


Figure S7. Housekeeping entropy production during one cycle (S34) as a function of δ . Here we set $r = 0.9$ and $\beta U_0 = 0.1$.

III. PROPERTIES OF THE ANDERSON MODEL

This section summarizes the properties of the Anderson model in greater detail. which consists of four subsections. In the first subsection, we summarize the evolution matrix and eigenstates in the Anderson model. In the second subsection, we present the explicit form of the density matrix. In the third subsection, we provide the explicit forms of the BSN connection and BSN curvature as well as the expansion coefficients. In the last subsection, we present some detailed calculations for the Anderson model. For simplicity, we do not write δ dependence of variables explicitly in this section.

A. Evolution matrix and eigenstates in the Anderson model

In this subsection, we summarize the evolution matrix and eigenstates in the Anderson model. A similar discussion can be found in Ref. [S1].

Because $\hat{\rho}$ is a diagonal matrix, $|\hat{\rho}\rangle$ also has only four components, and the transition matrix \hat{K} in Eq. (2) in the wideband approximation is given by the 4×4 matrix:

$$\hat{K} = - \begin{pmatrix} 2f_-^{(1)} & -f_+^{(1)} & -f_+^{(1)} & 0 \\ -f_-^{(1)} & f_-^{(0)} + f_+^{(1)} & 0 & -f_+^{(0)} \\ -f_-^{(1)} & 0 & f_-^{(0)} + f_+^{(1)} & -f_+^{(0)} \\ 0 & -f_-^{(0)} & -f_-^{(0)} & 2f_+^{(0)} \end{pmatrix}, \quad (\text{S36})$$

where we have introduced

$$f_+^{(j)} := f_L^{(j)} + f_R^{(j)}, \quad f_-^{(j)} := 2 - f_+^{(j)}, \quad (\text{S37})$$

with the Fermi distribution

$$f_\alpha^{(j)}(\mu_\alpha(\theta), U(\theta)) := \frac{1}{1 + e^{\beta(\epsilon_0 + jU(\theta) - \mu_\alpha(\theta))}} \quad (\text{S38})$$

in the lead $\alpha (= L \text{ or } R)$ for the single occupancy $j = 0$ and double occupancy $j = 1$.

It is straightforward to obtain the eigenvalues of $K(\Lambda(\theta))$ in Eq. (S36) as $\varepsilon_0 = 0$, $\varepsilon_1 = -f_+^{(0)} - f_-^{(1)}$, $\varepsilon_2 = -4 - \varepsilon_1$, $\varepsilon_3 = -4$. The left and right eigenfunctions corresponding to $\varepsilon_0 = 0$ for \hat{K} are given by

$$\langle \ell_0 | = (1, 1, 1, 1), \quad (\text{S39})$$

$$|r_0\rangle = \alpha_0 (f_+^{(0)} f_+^{(1)}, f_+^{(0)} f_-^{(1)}, f_+^{(0)} f_-^{(1)}, f_-^{(0)} f_-^{(1)})^T, \quad (\text{S40})$$

respectively, where $\alpha_0 = [2(f_+^{(0)} + f_-^{(1)})]^{-1}$ is the normalization factor. As discussed previously, the eigen state corresponding to the zero eigenvalue denotes the nonequilibrium steady state, namely $|r_0\rangle = |\hat{\rho}^{\text{ss}}\rangle$. Note that $|r_0\rangle$ satisfies $\langle \ell_0 | r_0 \rangle = \text{Tr} \hat{\rho}^{\text{ss}} = 1$. The left and right eigenfunctions corresponding to ε_1 , ε_2 , and ε_3 are respectively given by

$$\langle \ell_1 | = (f_-^{(1)}, \gamma, \gamma, -f_+^{(0)}), \quad (\text{S41})$$

$$|r_1\rangle = \alpha_1 (f_+^{(1)}, \gamma, \gamma, -f_-^{(0)})^T, \quad (\text{S42})$$

and

$$\langle \ell_2 | = (0, 1, -1, 0), \quad |r_2\rangle = \frac{1}{2}(0, 1, -1, 0), \quad (\text{S43})$$

and

$$\langle \ell_3 | = (f_-^{(0)} f_-^{(1)}, -f_-^{(0)} f_+^{(1)}, -f_-^{(0)} f_+^{(1)}, f_+^{(0)} f_+^{(1)}), \quad (\text{S44})$$

$$|r_3\rangle = \alpha_3 (1, -1, -1, 1)^T. \quad (\text{S45})$$

where $\alpha_1 = 2[(f_+^{(0)} + f_-^{(1)})(f_+^{(1)} + f_-^{(0)})]^{-1}$, $\alpha_3 = [2(f_-^{(0)} + f_+^{(1)})]^{-1}$, and $\gamma = (-f_+^{(0)} + f_-^{(1)})/2$.

B. Time evolution of the density matrix for the Anderson model

We are interested in the entropy production in the first cycle ΔS given by Eq. (5). For this purpose, we must know $\hat{\rho}(2\pi)$ and $\hat{\rho}(0)$. The former is given by

$$\begin{aligned} |\hat{\rho}(2\pi)\rangle &= |\hat{\rho}^{\text{ss}}(2\pi)\rangle + \sum_{i=1}^3 C_i |r_i(2\pi)\rangle \\ &= \begin{pmatrix} \alpha_0 f_+^{(0)} f_+^{(1)} + C_1 \alpha_1 f_+^{(1)} + C_3 \alpha_3 f_-^{(0)} f_-^{(1)} \\ \alpha_0 f_+^{(0)} f_-^{(1)} + C_1 \alpha_1 \gamma - C_3 \alpha_3 f_-^{(0)} f_+^{(1)} \\ \alpha_0 f_-^{(0)} f_-^{(1)} + C_1 \alpha_1 \gamma - C_3 \alpha_3 f_-^{(0)} f_+^{(1)} \\ \alpha_0 f_-^{(0)} f_+^{(1)} - C_1 \alpha_1 f_-^{(0)} + C_3 \alpha_3 f_+^{(0)} f_+^{(1)} \end{pmatrix}, \end{aligned} \quad (\text{S46})$$

where $\alpha_0 = [2(f_+^{(0)} + f_-^{(1)})]^{-1}$, $\alpha_1 = 2[(f_+^{(0)} + f_-^{(1)})(f_+^{(1)} + f_-^{(0)})]^{-1}$, $\alpha_3 = [2(f_-^{(0)} + f_+^{(1)})]^{-1}$, and $\gamma = (-f_+^{(0)} + f_-^{(1)})/2$.

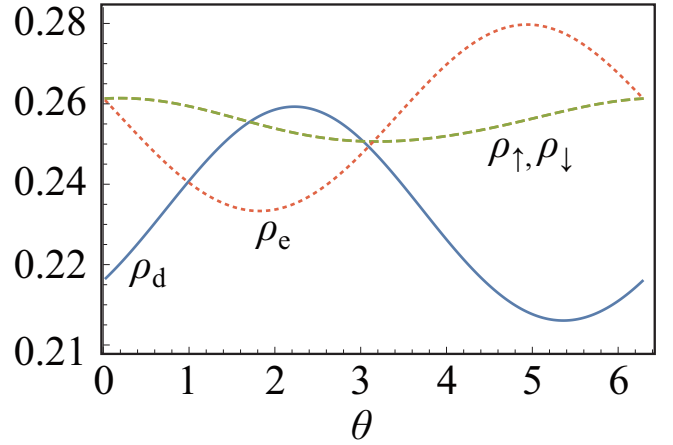


Figure S8. Time evolution of the elements of the density matrix.

Figure S8 plots the time evolution of the elements of $\hat{\rho}(\theta)$ as ρ_e , ρ_d , ρ_\uparrow and ρ_d . This figure clearly supports the positivity of all elements, therefore preserving the complete positivity argument.

C. BSN connection for Anderson model

In this subsection, we present an explicit form of the BSN connection for the Anderson model. For the explicit calculation of the BSN connection, we use Eqs. (6) and (7) with $\theta = 2\pi$. Integrating by parts, one obtains

$$\begin{aligned} &\int_0^{2\pi} \langle \tilde{\ell}_2(\phi) | \frac{d}{d\phi} |r_0(\phi)\rangle \\ &= \int_0^{2\pi} e^{\int_\phi^{2\pi} \varepsilon_2(\xi) \frac{d\xi}{\epsilon}} \langle \ell_2(\phi) | \frac{d}{d\phi} |r_0(\phi)\rangle \\ &= \int_0^{2\pi} e^{\int_\phi^{2\pi} \varepsilon_2(\xi) \frac{d\xi}{\epsilon}} \left[\frac{d}{d\phi} \langle \ell_2(\phi) | r_0(\phi) \rangle - \frac{d \langle \ell_2(\phi) |}{d\phi} |r_0(\phi)\rangle \right] \\ &= 0, \end{aligned} \quad (\text{S47})$$

where $\langle \ell_2(\phi) |$ is independent of ϕ . Thus, the summation of i in Eq. (6) is reduced to the summation with $i = 1$ and 3. The differentiation of $|r_0(\phi)\rangle$ with respect to ϕ

becomes

$$\begin{aligned}
& \frac{d}{d\phi} |r_0(\phi)\rangle \\
&= \left[\frac{d}{d\phi} \frac{1}{2(f_+^{(0)} + f_-^{(1)})} \right] \begin{pmatrix} f_+^{(0)} f_+^{(1)} \\ f_+^{(0)} f_-^{(1)} \\ f_+^{(0)} f_-^{(1)} \\ f_-^{(0)} f_-^{(1)} \end{pmatrix} \\
&+ \frac{1}{2(f_+^{(0)} + f_-^{(1)})} \frac{d}{d\phi} \begin{pmatrix} f_+^{(0)} f_+^{(1)} \\ f_+^{(0)} f_-^{(1)} \\ f_+^{(0)} f_-^{(1)} \\ f_-^{(0)} f_-^{(1)} \end{pmatrix} \\
&= \alpha(\Lambda) |r_0\rangle + \frac{1}{2(f_+^{(0)} + f_-^{(1)})} \frac{d}{d\phi} \begin{pmatrix} f_+^{(0)} f_+^{(1)} \\ f_+^{(0)} f_-^{(1)} \\ f_+^{(0)} f_-^{(1)} \\ f_-^{(0)} f_-^{(1)} \end{pmatrix}, \quad (\text{S48})
\end{aligned}$$

where $\alpha(\Lambda)$ is an unimportant factor because we are only interested in $\langle \ell_i(\phi) | \frac{d}{d\phi} |r_0(\phi)\rangle$ when $i \neq 0$ and $\langle \ell_i(\phi) | r_0(\phi)\rangle = 0$ for $i \neq 0$.

Substitution of Eq.(S48) into Eq.(6) with $\theta = 2\pi$ yields

$$|\hat{\rho}(2\pi)\rangle \simeq |r_0(2\pi)\rangle + \sum_{1,3} C_i |r_i(2\pi)\rangle, \quad (\text{S49})$$

$$C_i = - \int_0^{2\pi} d\phi \frac{\langle \tilde{\ell}_i(\phi) |}{2(f_+^{(0)} + f_-^{(1)})} \frac{d}{d\phi} \begin{pmatrix} f_+^{(0)} f_+^{(1)} \\ f_+^{(0)} f_-^{(1)} \\ f_+^{(0)} f_-^{(1)} \\ f_-^{(0)} f_-^{(1)} \end{pmatrix}. \quad (\text{S50})$$

By using $\frac{d}{d\theta}(f_+^{(j)} + f_-^{(j)}) = 0$, C_i becomes

$$\begin{aligned}
C_i &= - \int_0^{2\pi} d\phi \frac{\langle \tilde{\ell}_i(\phi) |}{2(f_+^{(0)} + f_-^{(1)})} \frac{df_+^{(0)}}{d\phi} \begin{pmatrix} f_+^{(1)} \\ f_-^{(1)} \\ f_-^{(1)} \\ -f_-^{(1)} \end{pmatrix} \\
&- \int_0^{2\pi} d\phi \frac{\langle \tilde{\ell}_i(\phi) |}{2(f_+^{(0)} + f_-^{(1)})} \frac{df_+^{(1)}}{d\phi} \begin{pmatrix} f_+^{(0)} \\ -f_+^{(0)} \\ -f_+^{(0)} \\ -f_-^{(0)} \end{pmatrix}. \quad (\text{S51})
\end{aligned}$$

Substituting Eq. (S41) into Eq. (S51), we obtain

$$\begin{aligned}
C_1 &= - \int_0^{2\pi} d\phi e^{\int_\phi^{2\pi} \varepsilon_1(\xi) \frac{d\xi}{\epsilon}} \frac{2f_-^{(1)}}{f_+^{(0)} + f_-^{(1)}} \frac{df_+^{(0)}}{d\phi} \\
&- \int_0^{2\pi} d\phi e^{\int_\phi^{2\pi} \varepsilon_1(\xi) \frac{d\xi}{\epsilon}} \frac{2f_+^{(0)}}{f_+^{(0)} + f_-^{(1)}} \frac{df_+^{(1)}}{d\phi}. \quad (\text{S52})
\end{aligned}$$

Similarly, we obtain

$$\begin{aligned}
C_3 &= \int_0^{2\pi} d\phi e^{\int_\phi^{2\pi} \varepsilon_3(\xi) \frac{d\xi}{\epsilon}} \frac{f_+^{(1)} f_-^{(1)}}{f_+^{(0)} + f_-^{(1)}} \frac{df_+^{(0)}}{d\phi} \\
&- \int_0^{2\pi} d\phi e^{\int_\phi^{2\pi} \varepsilon_3(\xi) \frac{d\xi}{\epsilon}} \frac{f_+^{(0)} f_-^{(0)}}{f_+^{(0)} + f_-^{(1)}} \frac{df_+^{(1)}}{d\phi} \\
&= \int_0^{2\pi} d\phi e^{4\epsilon^{-1}(\phi-2\pi)} \frac{f_+^{(1)} f_-^{(1)}}{f_+^{(0)} + f_-^{(1)}} \frac{df_+^{(0)}}{d\phi} \\
&- \int_0^{2\pi} d\phi e^{4\epsilon^{-1}(\phi-2\pi)} \frac{f_+^{(0)} f_-^{(0)}}{f_+^{(0)} + f_-^{(1)}} \frac{df_+^{(1)}}{d\phi}. \quad (\text{S53})
\end{aligned}$$

As shown by Eq. (S53), the factor $e^{4\epsilon^{-1}(\phi-2\pi)}$ in the integrand plays an important role. Owing to this factor, it is not necessary to consider the long-term memory in the dynamics. In the case of C_3 , the scaling factor does not depend on the choice of the trajectory, and only depends on θ . Thus, one can estimate the BSN curvature at ϕ .

For $\epsilon \ll 1$, the exponential factor $e^{4\epsilon^{-1}(\phi-2\pi)}$ behaves as the cut-off function and thus

$$\begin{aligned}
C_3 &\approx \int_{2\pi-\epsilon}^{2\pi} d\phi \left[\frac{f_+^{(1)} f_-^{(1)}}{f_+^{(0)} + f_-^{(1)}} \frac{df_+^{(0)}}{d\phi} - \frac{f_+^{(0)} f_-^{(0)}}{f_+^{(0)} + f_-^{(1)}} \frac{df_+^{(1)}}{d\phi} \right] \\
&\sim \epsilon \left[\frac{f_+^{(1)} f_-^{(1)}}{f_+^{(0)} + f_-^{(1)}} \frac{df_+^{(0)}}{d\phi} - \frac{f_+^{(0)} f_-^{(0)}}{f_+^{(0)} + f_-^{(1)}} \frac{df_+^{(1)}}{d\phi} \right]_{\phi=2\pi}. \quad (\text{S54})
\end{aligned}$$

Similarly, we can write

$$C_1 \sim \epsilon \left[\frac{2e^{\varepsilon_1(2\pi)}}{f_+^{(0)} + f_-^{(1)}} \left(f_-^{(1)} \frac{df_+^{(0)}}{d\phi} - f_+^{(0)} \frac{df_+^{(1)}}{d\phi} \right) \right]_{\phi=2\pi}. \quad (\text{S55})$$

From the above estimations, the leading order contribution of the geometrical phase is the order $O(\epsilon)$.

Let us show the C_3 reduces to zero in the non-interacting case $\beta U_0 = 0$. In this case, $f_\pm^{(0)} = f_\pm^{(1)} \equiv g_\pm$ and $g_+ + g_- = 2$; thus C_3 becomes

$$\lim_{\beta U_0 \rightarrow 0} C_3 = 0. \quad (\text{S56})$$

In the opposite limit $\beta U_0 \rightarrow \infty$ with $f_+^{(1)} = 0$, $f_-^{(1)} = 2$ C_3 also becomes zero, because

$$\lim_{\beta U_0 \rightarrow \infty} C_3 = 0. \quad (\text{S57})$$

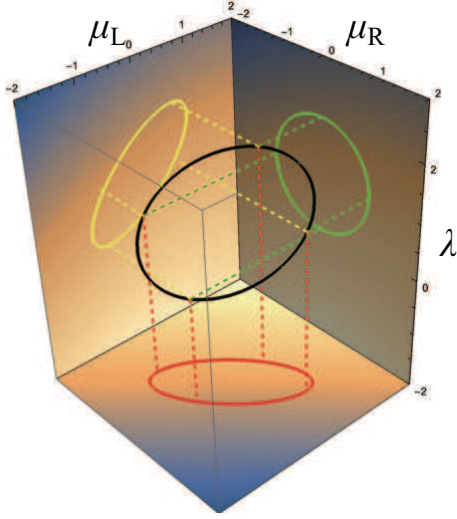


Figure S9. Schematic of control of parameters for $r = 1$ and $\delta = \pi/4$.

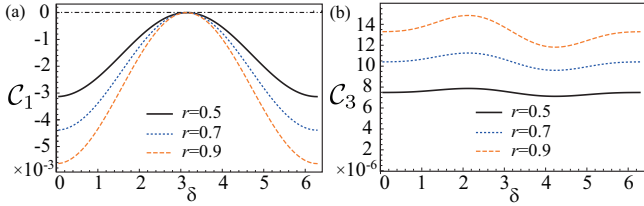


Figure S10. Plots of \mathcal{C}_1 (left figure) and \mathcal{C}_3 (right figure) versus δ for $r = 0.5, 0.7, 0.9$ with $\beta U_0 = 0.1$.

D. Some detailed results for the Anderson model

In this subsection, we present some detailed results beyond the main text, as well as a figure showing the control parameters in the parameter space.

First, Figure S9 shows a schematic of the control parameters in the parameter space for $r = 1$ and $\delta = \pi/4$.

In Fig. S10, we plot \mathcal{C}_1 (left figure) and \mathcal{C}_3 (right figure) versus δ for various r and $\beta U_0 = 0.1$. As shown, the coefficients increases as r increases. The coefficients \mathcal{C}_1 and \mathcal{C}_3 become zero at $\delta = \pi$.

Figure S11 shows coefficients \mathcal{C}_1 (left figure) and \mathcal{C}_3 (right figure) for various βU_0 and $r = 0.9$. As shown in Fig. S11, $|\mathcal{C}_i|$ with $i = 1$ and 3 increases with βU_0 .

We plot the one-cycle averaged relative entropy $\overline{S^{\text{HS}}}(\theta) := \frac{1}{2\pi} \int_{\theta}^{\theta+2\pi} d\phi S^{\text{HS}}(\hat{\rho}(\phi) || \hat{\rho}^{\text{SS}}(\phi))$ in Fig. S12 for $\delta = 0$, $r = 0.9$, and $\beta U_0 = 0.1$. This figure also indicates the oscillations of $\overline{S^{\text{HS}}}(\hat{\rho}(\theta) || \hat{\rho}^{\text{SS}}(\theta))$, which increase in some instances.

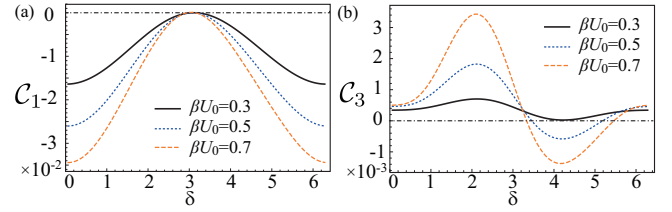


Figure S11. Plots of \mathcal{C}_1 (left figure) and \mathcal{C}_3 (right figure) versus δ for $\beta U_0 = 0.3, 0.5, 0.7$ with $r = 0.9$.

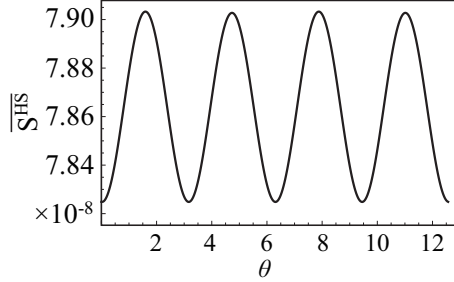


Figure S12. Sequential plots of time-averaged relative entropy $\overline{S^{\text{HS}}}(\theta)$ for $\delta = 0$, $r = 0.9$ and $\beta U_0 = 0.1$.

IV. DIFFERENCE BETWEEN REF. [S1] AND THE PRESENT STUDY

Most important difference between this paper and Ref. [S1] exists in the setup. Namely, we mainly discuss the relaxation process from NESS in this paper, but Ref. [S1] discussed the behavior after the system reaches a quasi-periodic state, in which the geometrical term can be ignored.

If we assume that $|\hat{\rho}(\theta)\rangle$ depends on θ only through modulation parameters Λ , as assumed in Ref. [S1], then we can express $|\hat{\rho}^{(1)}(\Lambda(\theta, \delta))\rangle := (\hat{\rho}(\theta, \delta) - \hat{\rho}^{\text{SS}}(\theta, \delta))/\epsilon$ as

$$|\hat{\rho}^{(1)}(\Lambda(\theta, \delta))\rangle = \hat{K}^+(\Lambda(\theta, \delta)) \frac{d}{d\theta} |\hat{\rho}^{\text{SS}}(\Lambda(\theta, \delta))\rangle \quad (\text{S58})$$

which is the equation used in Ref. [S1].

However, if $|\hat{\rho}(\theta, \delta)\rangle$ explicitly depends on θ and the geometrical term still survives, it is dangerous to use Eq. (S58). To clarify this difference, consider the relaxation process in the absence of the parameter modulation, in which the time evolution of the density matrix is given by

$$\begin{aligned} |\hat{\rho}(\theta, \delta)\rangle &= |\hat{\rho}^{\text{SS}}\rangle + \sum_{i \neq 0} e^{\int_0^\theta d\theta \frac{\epsilon_i}{\epsilon}} |r_i\rangle \\ &= |\hat{\rho}^{\text{SS}}\rangle + \sum_{i \neq 0} e^{\frac{\epsilon_i}{\epsilon} \theta} |r_i\rangle \\ &= |\hat{\rho}^{\text{SS}}\rangle + \sum_{i \neq 0} e^{-\frac{|\epsilon_i|}{\epsilon} \theta} |r_i\rangle. \end{aligned} \quad (\text{S59})$$

In this case, the density matrix relaxes to the steady state $|\hat{\rho}^{\text{SS}}\rangle$ in the long time limit $\theta/\epsilon \gg 0$. We note that this

limit is usually achieved not by $\theta \gg 1$ but by $\epsilon \rightarrow 0$. It is obvious that $\epsilon \rightarrow 0$ is the singular limit and the expansion via ϵ is not available because the convergence radius

of $e^{-1/x}$ is zero. Thus, if the density matrix explicitly depends on θ , it is dangerous to use the naive perturbation via ϵ used in Ref. [S1].

-
- [S1] H. Hayakawa, V. M. M. Paasonen, and R. Yoshii, “Geometrical Quantum Chemical Engine”, arXiv:2112.12370 (2021).
- [S2] T. Sagawa and H. Hayakawa, Geometrical expression of excess entropy production, Phys. Rev. E **84**, 051110 (2011).
- [S3] T. Yuge, T. Sagawa, A. Sugiura, and H. Hayakawa, Geometrical Excess Entropy Production in Nonequilibrium Quantum Systems, J. Stat. Phys. **153**, 412 (2013).
- [S4] R. Yoshii and H. Hayakawa, “Analytical expression of geometrical pumping for a quantum dot based on quantum master equation”, arXiv:1312.3772